Ir-CPI, a coagulation contact phase inhibitor from the tick *Ixodes ricinus*, inhibits thrombus formation without impairing hemostasis

Yves Decrem,[1] Géraldine Rath,[2] Virginie Blasioli,[1] Philippe Cauchie,[3] Séverine Robert,[4] Jérôme Beaufays,[1] Jean-Marie Frère,[5] Olivier Feron,[2] Jean-Michel Dogné,[4] Chantal Dessy,[2] Luc Vanhamme,[1,6] and Edmond Godfroid[1]

[1]Service de Biologie Moléculaire des Ectoparasites, Institut de Biologie et Médecine Moléculaires, Université Libre de Bruxelles, Gosselies B-6041, Belgium
[2]Unit of Pharmacology and Therapeutics (FATH 5349), Université Catholique de Louvain, Brussels B-1200, Belgium
[3]Experimental Medecine Laboratory, Université de Bruxelles, Montigny-Le-Tilleul B-6110, Belgium
[4]Department of Pharmacy, Facultés Universitaires Notre Dame de la Paix Namur, B-5000, Belgium
[5]Centre d'Ingénierie des Protéines, Institut de Chimie B6a, Université de Liège, B-4000 Liège, Belgium
[6]Service de Parasitologie Moléculaire, Institut de Biologie et Médecine Moléculaires, Université Libre de Bruxelles, Gosselies B-6041, Belgium

Blood coagulation starts immediately after damage to the vascular endothelium. This system is essential for minimizing blood loss from an injured blood vessel but also contributes to vascular thrombosis. Although it has long been thought that the intrinsic coagulation pathway is not important for clotting in vivo, recent data obtained with genetically altered mice indicate that contact phase proteins seem to be essential for thrombus formation. We show that recombinant *Ixodes ricinus* contact phase inhibitor (Ir-CPI), a Kunitz-type protein expressed by the salivary glands of the tick *Ixodes ricinus*, specifically interacts with activated human contact phase factors (FXIIa, FXIa, and kallikrein) and prolongs the activated partial thromboplastin time (aPTT) in vitro. The effects of Ir-CPI were also examined in vivo using both venous and arterial thrombosis models. Intravenous administration of Ir-CPI in rats and mice caused a dose-dependent reduction in venous thrombus formation and revealed a defect in the formation of arterial occlusive thrombi. Moreover, mice injected with Ir-CPI are protected against collagen- and epinephrine-induced thromboembolism. Remarkably, the effective antithrombotic dose of Ir-CPI did not promote bleeding or impair blood coagulation parameters. To conclude, our results show that a contact phase inhibitor is an effective and safe antithrombotic agent in vivo.

CORRESPONDENCE
Edmond Godfroid:
Edmond.Godfroid@ulb.ac.be

Abbreviations used: ANOVA, analysis of variance; aPTT, activated partial thromboplastin time; cDNA, complementary DNA; GST, glutathione *S*-transferase; HK, high molecular weight kininogen; Ir-CPI, *Ixodes ricinus* contact phase inhibitor; IVC, inferior vena cava; PL, phospholipid; PPP, platelet-poor plasma; PT, prothrombin time; RU, resonance unit; TF, tissue factor; t-PA, tissue plasminogen activator.

The classical cascade of coagulation describes two converging enzymatic cascades that are triggered either by exposure of blood to a damaged vessel wall (the extrinsic pathway) or by blood-borne components of the vascular system (the intrinsic pathway). In fact, the extrinsic coagulation pathway starts by the binding of FVII (plasma factor VII) to tissue factor (TF) produced by subendothelial cells. The resulting complex activates FX (factor X), which leads to thrombin generation and, ultimately, initiates the process of fibrin formation (Davie and Ratnoff, 1964; MacFarlane, 1964). In contrast, the intrinsic pathway is initiated by contact phase proteins, including the zymogens factor XII, factor XI, and prekallikrein, as well as the cofactor high molecular weight kininogen (HK; Yarovaya et al., 2002). FXII undergoes autoactivation when bound to polyanionic surfaces, generating activated factor XII by a conformational change (Silverberg et al., 1980; Tankersley and Finlayson, 1984). FXIIa then converts prekallikrein into kallikrein by cleavage of a single peptide bond. Once small amounts of kallikrein are formed, they catalyze the conversion of surface-bound FXII into FXIIa,

The Rockefeller University Press $30.00
J. Exp. Med. Vol. 206 No. 11 2381-2395
www.jem.org/cgi/doi/10.1084/jem.20091007

leading to strong positive feedback on the system (Cochrane et al., 1973; Dunn et al., 1982). During this process, FXII is activated by a succession of proteolysis steps leading to the production of a series of different active enzymes: FXIIa and FXIIf (Kaplan and Austen, 1971; Revak et al., 1977; Silverberg et al., 1980; Dunn and Kaplan, 1982). In vitro, the contact phase system initiates the intrinsic coagulation pathway by cleavage of FXI into activated factor XI by FXIIa (Bouma and Griffin, 1977; Kurachi and Davie, 1977). FXIIf may also activate FVII, the proenzyme initiating the extrinsic coagulation pathway (Kisiel et al., 1977; Radcliffe et al., 1977). Propagation of clotting involves several positive-feedback mechanisms. For example, thrombin can activate FXI, which activates additional factor IX, therefore amplifying the coagulation process (von dem Borne et al., 1995). The surface-associated FVIIa–TF complex can activate FIX in addition to FX. This activation loop provides an important contribution to the blood clotting process (Josso and Prou-Wartelle, 1965; Osterud and Rapaport, 1977; Bauer et al., 1990). It later became clear that activation of the contact–phase system is critically involved in proteolytic mechanisms distinct from coagulation, namely the kallikrein–kinin, complement, and fibrinolytic systems (Mandle and Kaplan, 1979; Ghebrehiwet et al., 1983; Kaplan et al., 2002; Moreau et al., 2005).

The search for new anticoagulants is a major challenge in medicine. In practice, this involves identifying drugs capable of preventing thrombus formation without increasing the risk of hemorrhage. For the past 40 yr, anticoagulant treatment has been dominated by two classes of agents: heparins and antivitamins K. Heparins accelerate the inhibitory action of antithrombin on some activated coagulation factors (specifically FXa and thrombin) by indirect inhibition of these factors and are only active when administered parenterally. The latter prevent the final synthesis of four coagulation factors (prothrombin, FVII, FIX, and FX). These compounds require careful laboratory testing to guarantee sufficient antithrombotic effectiveness while avoiding the risk of hemorrhage. This disadvantage, together with the relatively narrow therapeutic margin of these drugs, has considerably stimulated research into other types of agents. The choice of anticoagulant therapy, either for venous thromboembolism or arterial thrombosis (myocardial infarction or stroke), is based on how well a drug inhibits thrombosis and its hemorrhagic side effects. The recent discovery that FXI and FXII deficiency protects against thrombosis without causing spontaneous bleeding in mice makes FXII a unique and ideal target for drug design (Gailani and Renné, 2007; Renné and Gailani, 2007). Indeed, FXII-deficient mice were found to be protected against arterial thrombosis, collagen- and epinephrine-induced thromboembolism (Renné et al., 2005), and ischemic brain stroke (Kleinschnitz et al., 2006). In all these models, the protection was abolished by the infusion of human FXII into FXII-null mice. Moreover, as in the case of their human counterparts, the FXII-null mice do not suffer from impaired hemostasis (Pauer et al., 2004).

Many blood-sucking ectoparasites synthesize substances to thwart the defense mechanisms of the hosts on which they feed (Ribeiro and Francischetti, 2003). Ticks, in particular, produce salivary substances capable of modulating the host immune responses and maintain blood in a sufficiently fluid state to effectively acquire and digest their blood meal (Brossard and Wikel, 2004). As indicated earlier, hemostasis involves a network of factors organized in different pathways that can be activated independently. Ticks are, therefore, confronted with a redundant system and must simultaneously block several different steps to obtain effective antihemostasis. This has been achieved during the long tick–host coevolution, as ticks produce a variety of compounds with antihemostatic activity (Ribeiro and Francischetti, 2003; Brossard and Wikel, 2004; Steen et al., 2006).

In this study, we characterize a novel serine protease inhibitor from the tick *Ixodes ricinus*. This protein, *Ixodes ricinus* contact phase inhibitor (Ir-CPI), has one Kunitz domain and is capable of effectively inhibiting the intrinsic coagulation pathway and, to a much lesser extent, fibrinolysis in vitro. We also showed that Ir-CPI can inhibit the reciprocal activation of FXII, prekallikrein, and FXI in human plasma by specifically binding to these three factors when they are activated. Lastly, tests in animal models showed that Ir-CPI has antithrombotic properties in vivo and inhibits the formation of both venous and arterial thrombi without disturbing the clotting balance. To our knowledge, this is the first time that a selective inhibitor of the coagulation contact phase has been shown to protect against the formation of both venous and arterial thrombi.

RESULTS

Sequence analysis of Seq7

Expression and purification of recombinant Seq7. To identify complementary DNAs (cDNAs) coding for proteins specifically expressed in the salivary glands of female *I. ricinus* ticks, a subtractive cDNA library was set up using messenger RNAs extracted from salivary glands of unfed and 5-d-fed female *I. ricinus* ticks (Leboulle et al., 2002). One clone, formerly called *seq*7 (GenBank accession no. AJ269641), was selected for further characterization as it coded for a predicted protein (Seq7) with similarities to the second Kunitz domain of human TF pathway inhibitor. The predicted Seq7 amino acid sequence comprised the typical consensus Kunitz motif F-x(3)-G-C-x(6)-[FY]-x(5)-C. Moreover, SignalP and TargetP programs predicted a signal peptide cleavage site at position 23 and the absence of a hydrophobic transmembrane region, suggesting that the protein was secreted.

To produce a recombinant form of Seq7, the open reading frame deleted from the sequence predicted to code for a signal peptide was cloned in the expression vector pGEX-6P-1 in frame with the coding sequence of glutathione *S*-transferase (GST) and expressed in bacteria. Affinity purification followed by cleavage with PreScission protease and further fast protein liquid chromatography yielded pure recombinant protein (unpublished data).

Recombinant Ir-CPI prolongs activated partial thromboplastin time (aPTT) and fibrinolysis time. As Seq7 displayed homology to a factor involved in hemostasis, the activity of the recombinant protein was first assessed using classical global hemostasis tests in vitro. The recombinant protein had no effect on PFA closure time or platelet aggregation with whole blood (unpublished data). This suggested that Seq7 did not interfere with primary hemostasis. The anticoagulant activity of Seq7 was then assessed using four routine tests of plasma clotting time. Prothrombin, thrombin, and RVV times remained unchanged (unpublished data), suggesting that Seq7 did not interfere with extrinsic or common factors of the coagulation cascade. However, recombinant Seq7 prolonged aPTT (7.7 times at 2 μM) in a dose-dependent manner (Fig. 1 A), showing interference with the intrinsic pathway. Finally, the activity of Seq7 was investigated on fibrinolysis. The results showed that the fibrinolysis time was slightly increased by 1.18-fold in the presence of Seq7 at 2 μM (Fig. 1 B). All these experiments were also performed with GST used as a negative control. No interference was observed with any of the tests (unpublished data). According to these results, Seq7 was renamed Ir-CPI (*Ixodes ricinus* contact phase inhibitor).

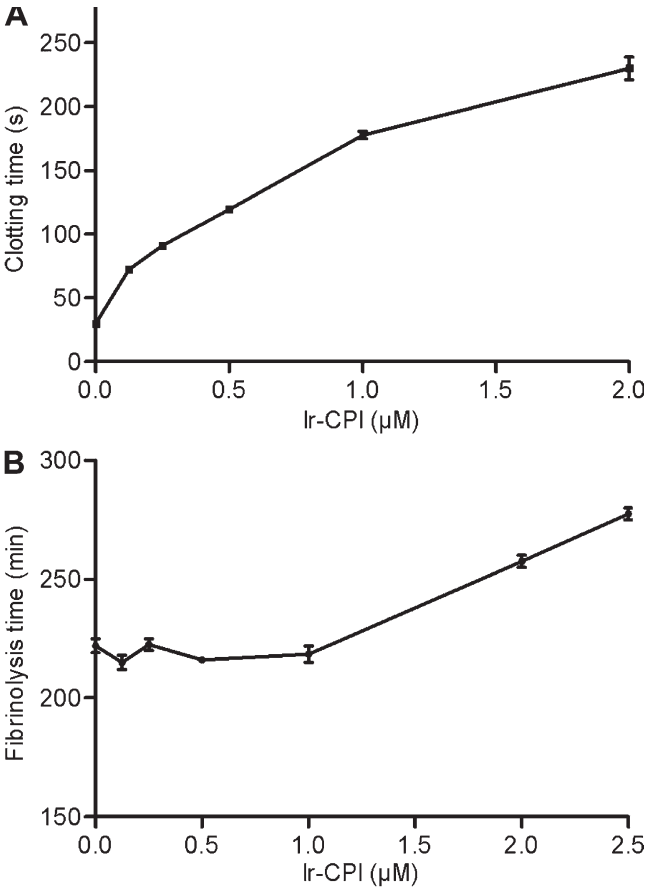

Figure 1. In vitro anticoagulant activity of Ir-CPI. Increasing amounts of Ir-CPI were incubated with human plasma for 2 min. Coagulation aPTT (A) and clot lysis times (B) were determined as described in Materials and methods. Each point represents the mean ± SEM of three independent determinations.

Ir-CPI inhibits thrombin generation

As thrombin is the key player in clot formation, the effects of Ir-CPI were investigated on its activity during the coagulation process. The intrinsic coagulation pathway was induced using a mixture of ellagic acid and phospholipid (PLs) as triggers. The addition of recombinant Ir-CPI to the assay caused a dose-dependent prolongation of the lag time and a dose-dependent decrease in the peak concentration of active thrombin (Cmax) compared with the control curve (i.e., without inhibitor; Fig. 2 A). At a final Ir-CPI concentration of 9.1 μM, the lag time was prolonged 3.6-fold compared with the control curve. Regarding Cmax, the effect was maximal at 0.7 μM and did not increase at higher concentrations (2.2 μM, 6.6 μM, and 9.1 μM). At a concentration of 0.7 μM,

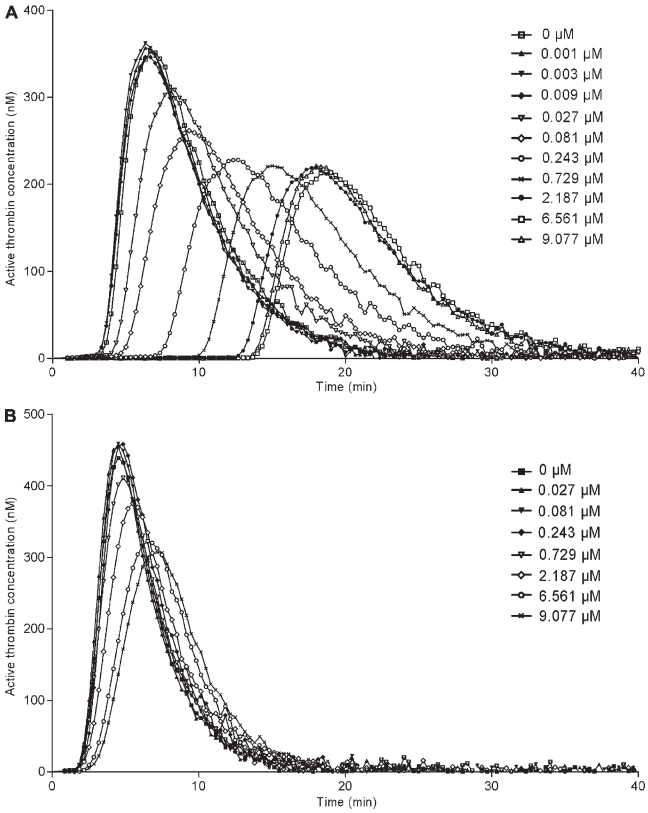

Figure 2. Effect of Ir-CPI on the thrombin activity profile during the coagulation process induced either by intrinsic or extrinsic coagulation pathway. (A) Human plasma was incubated with various concentrations of Ir-CPI (0, 0.001, 0.003, 0.009, 0.027, 0.081, 0.243, 0.729, 2.187, 6.561, and 9.077 μM), and the mixture was activated with ellagic acid and PL to initiate the intrinsic coagulation pathway. (B) Human plasma was incubated with various concentrations of Ir-CPI (0, 0.729, 2.187, 6.561, and 9.077 μM), and the mixture was activated with 5 pM TF and PL to initiate the extrinsic coagulation pathway. The amidolytic activity of thrombin was determined by adding its specific fluorogenic substrate and recording the increase in fluorescent signal. Results are presented as the mean of three independent experiments.

the Cmax was reduced by 37% and the lag time was prolonged 2.7-fold.

In contrast, when the coagulation cascade was triggered by the extrinsic pathway (5 pM TF and 4 μM PL), a slight dose-dependent decrease in Cmax and a dose-dependent prolongation of the lag time were observed (Fig. 2 B). At a final Ir-CPI concentration of 9.1 μM, the Cmax was reduced by 30% and the lag time was prolonged 1.6-fold. Similar results were obtained when a lower concentration of TF (1 pM) and PL (4 μM) were used as triggers. Overall, these results show that Ir-CPI is an inhibitor of thrombin generation.

Ir-CPI inhibits the activation of contact system factors

To determine the targets of Ir-CPI, its effect on seven procoagulant active serine proteases (namely kallikrein, FXIIa, FXIa, FIXa, FXa, FIIa, and FVIIa) and two fibrinolytic serine proteases (tissue plasminogen activator [t-PA] and plasmin) was measured in amidolytic tests using specific substrates for each of these serine proteases. These assays failed to reveal any effect of the Ir-CPI protein on the amidolytic activity of these factors (unpublished data).

The capacity of Ir-CPI protein to inhibit the activation of these factors was then analyzed on human plasma contact phase factors by incubating human plasma with Ir-CPI and then adding a contact phase activator. The activation of contact factors (FXII, FXI, and kallikrein) was evaluated using a specific substrate for each factor. The results showed that Ir-CPI inhibited the generation of the active form of these three factors in a dose-dependent manner (Fig. 3 A).

The effect of Ir-CPI on contact phase factors was further dissected and examined in reconstituted systems using purified factors and their specific chromogenic substrates. In each of these assays, we compared the activation of a nonactivated factor (zymogen) by an activated factor in the presence or absence of Ir-CPI. The results showed that Ir-CPI inhibited the activation of prekallikrein into kallikrein by FXIIa, activation of FXI into FXIa by FXIIa, and activation of FXII into FXIIa by FXIa (Fig. 3, B–D). In contrast, Ir-CPI failed to inhibit the activation of FXII into FXIIa by kallikrein (unpublished data). Collectively, the results of these experiments show that Ir-CPI impacts the activation of some factors (e.g., FXIa and FXIIa) participating in the contact phase of coagulation.

Ir-CPI binds to FXIa, FXIIa, kallikrein, and plasmin

We then asked whether the inhibitory activity of Ir-CPI involved a direct interaction with one or more blood coagulation factors by evaluating the capacity of Ir-CPI to bind to coagulation or fibrinolysis factors or cofactors by surface plasmon resonance. The assays demonstrated a specific interaction between Ir-CPI and four factors: FXIIa, FXIa, plasmin, and kallikrein (Fig. 4). No interaction was observed with any of the other factors or cofactors tested (prekallikrein, HK, FXII, FXI, FIX, FIXa, FX, FXa, prothrombin, thrombin, FVIIa, t-PA, and plasminogen; unpublished data). Except for kallikrein, these data were confirmed by using dot blot assays (Fig. S1). Moreover, the kinetics of interaction between Ir-CPI and the four targeted factors (FXIIa, FXIa, plasmin, and kallikrein) were measured after immobilization of Ir-CPI. In assays designed to determine the binding kinetics, the quantity of immobilized Ir-CPI was deliberately kept at a low level (~200 resonance units [RU]) to avoid problems caused by limitation of the reaction rate by a mass-transport effect. The initial binding rate was shown to

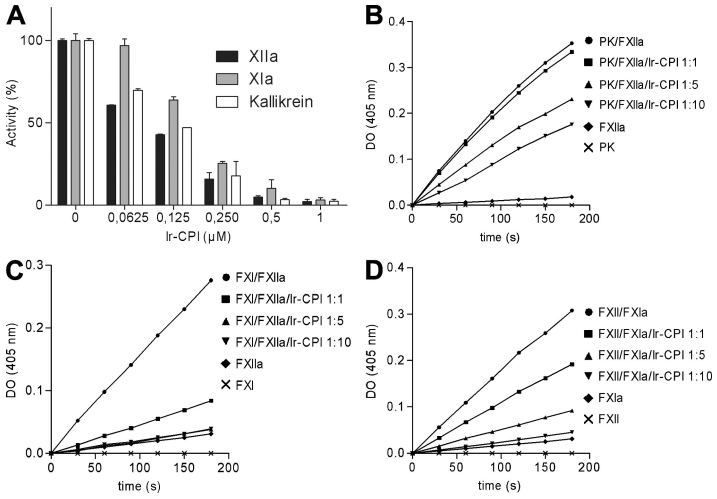

Figure 3. Inhibitory effect of Ir-CPI on generation of FXIIa, FXIa, and kallikrein in human plasma and on reconstituted systems. (A) Diluted human plasma was incubated with various concentrations of Ir-CPI (0.0625, 0.125, 0.25, 0.5, and 1 μM), and the mixture was activated with aPTT reagent to initiate the contact system. The amidolytic activities of generated FXIIa, FXIa, and kallikrein were determined by adding their specific chromogenic substrates and recording the increase in absorbance at 405 nm. (B–D) The effect of Ir-CPI was examined in reconstituted systems using purified factors and their specific chromogenic substrates. The activation of a nonactivated factor by an activated factor, in the presence or absence of Ir-CPI, was analyzed in each experiment. (B) Activation of prekallikrein into kallikrein by FXIIa. (C) Activation of FXI into FXIa by FXIIa. (D) Activation of FXII into FXIIa by FXIa Results are presented as the mean ± SEM of three independent determinations.

Table I. Kinetic constants for Ir-CPI interactions with kallikrein, FXIa, FXIIa, and plasmin

Ir-CPI–targeted factors	k_{a1} (1/Ms)	k_{d1} (1/s)	k_{a2} (1/s)	k_{d2} (1/s)	K (1/M)
Kallikrein	$3.49 \pm 0.54 \times 10^{4}$	$5.32 \pm 0.92 \times 10^{-2}$	$8.34 \pm 0.07 \times 10^{-3}$	$1.42 \pm 0.11 \times 10^{-3}$	$4.51 \pm 0.19 \times 10^{6}$
FXIa	$2.31 \pm 0.59 \times 10^{6}$	$1.02 \pm 0.51 \times 10^{-1}$	$2.98 \pm 0.29 \times 10^{-2}$	$2.32 \pm 0.28 \times 10^{-3}$	$3.83 \pm 2.37 \times 10^{8}$
FXIIa	$2.19 \pm 0.06 \times 10^{5}$	$9.46 \pm 0.04 \times 10^{-2}$	$6.55 \pm 0.66 \times 10^{-1}$	$1.05 \pm 0.04 \times 10^{-1}$	$1.68 \pm 1.10 \times 10^{8}$
Plasmin	$9.00 \pm 0.39 \times 10^{5}$	$5.35 \pm 1.33 \times 10^{-3}$	$5.82 \pm 0.99 \times 10^{-3}$	$6.14 \pm 0.96 \times 10^{-3}$	$3.30 \pm 0.57 \times 10^{8}$

Data represent the mean ± SD of three experiments.

be independent of flow variations by linear regression measurements at the start of kinetics with injections of analytes at increasing flows from 30 to 70 µl/min. This confirmed that there was no limitation of the reaction (unpublished data). Interaction kinetics were determined for each analyte at six different concentrations (from 5 to 300 nM). The data were processed with the BIA evaluation software and the best fits obtained with the following two-state binding model, which implies the binding of the plasma protein to immobilized Ir-CPI in a 1/1 ratio followed by a reversible conformation change:

$$A + B \underset{k_{d1}}{\overset{k_{a1}}{\leftrightarrow}} AB \underset{k_{d2}}{\overset{k_{a2}}{\leftrightarrow}} (AB),$$

where A is the plasma protein, B is the immobilized Ir-CPI, and (AB) is the complex form after conformational change in the initial complex AB. In this model, k_{a1} and k_{d1} are the association and dissociation rate constants for the formation of AB, and k_{a2} and k_{d2} the forward and backward rate constants for the AB↔(AB) conformation change. The values of these rate constants are shown in Table I. These results indicate that Ir-CPI specifically binds to FXIIa, FXIa, kallikrein, and plasmin but not to their zymogenic forms (Fig. 4). It should, however, be noted that the values in Table I are only indicative of the orders of magnitude. Indeed, large variations of the constants are observed when the association curves (Fig. 5, 0–84 s) are analyzed individually. Similarly, when the dissociation curves are fitted to a sum of two exponentials ($y = y_f + Ae^{-k't} + Be^{-k''t}$, where t is the time and k′ and k′′ are complex functions of k_{a1}, k_{a2}, k_{d1}, and k_{d2}), the best fits are obtained with nonzero values of y_f. This indicates that, with two exponentials, dissociation is not complete when time increases, which suggests a third, irreversible or very slowly reversible, step after the AB ↔(AB) conformation change. This irreversible component represents 20–40% for kallikrein, 53–60% for fXIa, 10–24% for fXIIa, and 19–27% for plasmin.

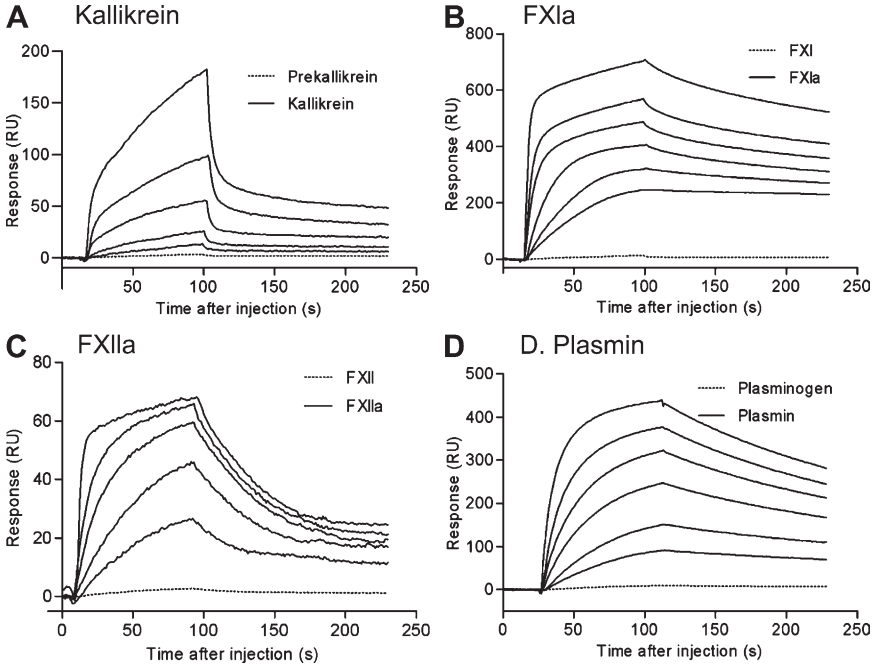

Figure 4. Sensorgrams for interactions between targeted factors (kallikrein, FXIa, FXIIa, and plasmin) and immobilized Ir-CPI measured by surface plasmon resonance. Ir-CPI was immobilized on the surface of a CM5 sensor chip at a level of 200 RU. Factors (from 5 to 300 nM) were injected at a flow rate of 70 µl/min in HBS buffer, and association was monitored for 84 s. After return to buffer flow, dissociation was monitored for 150 s. The sensor chip surface was regenerated by a pulse injection of 25 mM NaOH after each experiment. For each interaction, one representative result from three independent determinations is shown.

Ir-CPI interferes with thrombus formation in animal models of venous thrombosis

Before testing the antithrombotic action of Ir-CPI, we evaluated the half-life of Ir-CPI in vivo. A semiquantitative estimate of Ir-CPI pharmacokinetics was obtained using ^{125}I-Ir-CPI. The results showed that plasma ^{125}I-Ir-CPI concentrations were ~40.8 ± 9.9% of the maximum value 20 h after i.v. administration of the recombinant protein (unpublished data). The anticoagulant effect of Ir-CPI was also investigated with plasma from rats and mice. The results showed that Ir-CPI prolongs both the rat and the mouse aPTT by 2.18- and 2.77-fold at 2 μM, respectively.

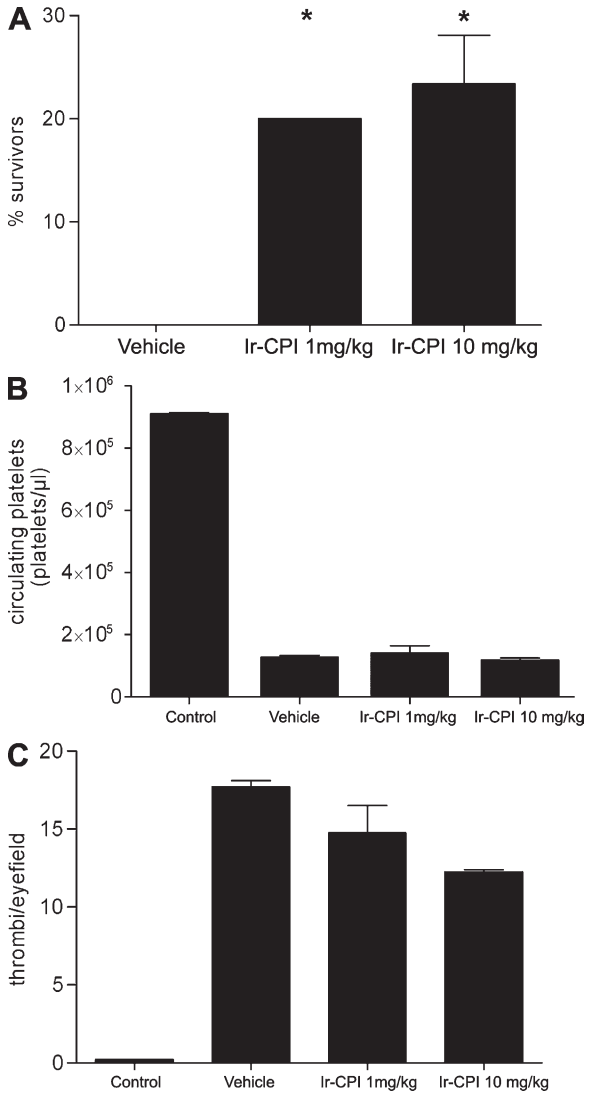

Figure 5. Effect of Ir-CPI on pulmonary embolism model. (A) Mortality associated with i.v. of collagen and epinephrine after administration of PBS (vehicle) or Ir-CPI. All PBS-treated mice died within 5 min. Animals alive 30 min after the challenge were considered survivors. Data represent the mean ± SEM of the results obtained with 15 animals per group from two independent experiments. *, $P \leq 0.05$. (B) Platelet counts in mice 2 min after infusion of collagen/epinephrine. The control group was not injected with collagen/epinephrine. Data represents the mean ± SEM of results obtained with five animals per group from two independent experiments. Values on the number of circulating platelets in the three groups of injected mice are significantly alike. (C) Number of thrombi in the lungs of mice 2 min after infusion of collagen/epinephrine. Thrombi per visual field were counted at 20×. Data represent the mean for 20 fields per mice ($n = 3$ per group) from two independent experiments.

The antithrombotic in vivo action of Ir-CPI was first evaluated in a mouse model of lethal pulmonary thromboembolism, induced by the infusion of a mixture of collagen and epinephrine. All vehicle mice (15 out of 15) died within 5 min, with a dramatic reduction in circulating platelet counts within 2 min of the challenge (Fig. 5, A and B). In contrast, the two groups of Ir-CPI–treated mice showed a significant increase of survivors (3 out of 15 [20%] at 1 mg/kg Ir-CPI and 4 out 15 [26.7%] at 10 mg/kg Ir-CPI), although their peripheral platelet counts were reduced to a similar degree as those of mice injected with PBS. This suggests that the protection conferred by Ir-CPI administration is not caused by a platelet adhesion/activation defect but by a defect in thrombin generation or some other FXIIa/FXIa-related activity. Consistent with this premise, the analysis of the effect of Ir-CPI on primary hemostasis by using plasma and total blood from Ir-CPI–treated mice demonstrated no effect of Ir-CPI on platelet aggregation (unpublished data). In addition, the examination of histological sections of lung tissue showed a reduction in the number of occluded vessels in Ir-CPI–treated mice (survivors and nonsurvivors), whereas the majority of vessels were obstructed in vehicle (Fig. 5 C).

The effect of Ir-CPI on venous thrombus formation was then assessed using two thrombosis animal models. In the first model in rats, venous thrombosis was induced by stasis after vessel ligation and activation of thrombosis by severe endothelial damage and vessel occlusion with ferric chloride (see Materials and methods). The control group showed 100% thrombus formation, with a mean thrombus weight of 19.6 ± 1.6 mg/kg ($n = 6$). In contrast, prior i.v. administration of Ir-CPI induced a dose-dependent progressive decrease in thrombus formation, with a calculated effective concentration (EC50) at 49.2 μg/kg and with a maximum effect starting at 100 μg/kg (Fig. 6 A).

The efficacy of Ir-CPI in inhibiting thrombus formation was also measured on a murine model of venous thrombosis in which complete stasis is induced by ligation of the inferior vena cava (IVC). 5 min before surgery, mice were given an i.v. injection of either Ir-CPI (1 or 10 mg/kg) or the vehicle (PBS) in the caudal vein. Mice were sacrificed 24 h after thrombosis induction and the thrombosed IVC fragments were harvested and weighed. The clot weight/body weight ratio was significantly reduced in the presence of Ir-CPI, from 0.70 ± 0.11 in the control group to 0.24 ± 0.06 in the group of mice treated preventively with Ir-CPI at a dose of 1 mg/kg (Fig. 6 B). Moreover, the clot weight/clot length ratio was 2.83 ± 0.54 for a thrombus formed in the control group, whereas it was only 1.86 ± 0.13 in mice treated with a dose of 1 mg/kg of Ir-CPI (Fig. 6 C). At a dose of 10 mg/kg of Ir-CPI, the clot weight/body weight and the clot weight/

Table II. Hemostasis and coagulation in Ir-CPI–treated rats

Inhibitors	aPTT	PT	Fibrinolysis	Bleeding effect (O.D. 450 nm)
	s	*s*	*min*	
PBS	20.0 ± 3.8	21.4 ± 1.5	53 ± 27	0.026 ± 0.006
Ir-CPI 0.1 mg/kg	20.7 ± 3.9	21.3 ± 1.1	66 ± 29	0.067 ± 0.060
Ir-CPI 1 mg/kg	28.8 ± 3.4[a]	21.6 ± 1.6	51 ± 28	0.021 ± 0.008
LMWH 0.5 mg/kg	36.2 ± 3.8[a]	26.9 ± 1.4[a]	57 ± 19	0.174 ± 0.091[a]

Values are mean ± SEM (n = 5 for each test). LMWH, low molecular weight heparin.
[a]$P < 0.05$, as compared to values observed in the control (PBS) by one-way ANOVA and Student's t test–Newman-Keuls test.

clot length ratios reached 0.15 ± 0.11 and 1.60 ± 0.33, respectively. We also performed time-course experiments of clot formation in untreated and Ir-CPI treated mice. In Ir-CPI 1 mg/kg-treated mice, the clot weight/body weight ratio and the clot weight/clot length ratio were significantly lower than in untreated mice after 6, 16, and 24 h stasis, whereas no difference was observed after 2 and 4 h. (Fig. 6, D and E).

To examine the effect of Ir-CPI on blood coagulation parameters after i.v. administration, the effects of Ir-CPI were then tested on ex vivo clotting assays. For the rats, Table II shows that aPTT values were similar in comparison with controls for Ir-CPI EC50 and 100-μg/kg doses, whereas aPTT values were statistically higher in comparison with controls for Ir-CPI doses >1 mg/kg, showing a ∼1.4-fold increase in the latter case. In contrast, prothrombin time (PT) was not affected by 1 mg/kg Ir-CPI. Moreover, this high dose of Ir-CPI had no effect on the fibrinolysis time (Table II). Finally, the bleeding effect of Ir-CPI was evaluated using a tail-transection model. No statistically significant blood loss was observed 5 min after administration of 1 mg/kg Ir-CPI (Table II).

The effects of Ir-CPI in mice on ex vivo clotting assays were also tested. These showed that Ir-CPI at a dose of 1 mg/kg did not modify aPTT, PT, and fibrinolysis times. However, aPTT was increased in the presence of Ir-CPI at a dose of 10 mg/kg (21.7 ± 2.4 in the control group vs. 39.8 ± 5.2 in the group of Ir-CPI–treated mice), whereas PT and fibrinolysis times remain unchanged at this dose. Finally, the bleeding effect of Ir-CPI was also evaluated by using a tail-transection model. In this case, the bleeding time was not affected after administration of 1 mg/kg Ir-CPI. Although we observed a slight increased of the bleeding time at a dose of 10 mg/kg, this value was not significant as compared with those obtained with untreated mice (Table III). Taken as a whole, these results show that Ir-CPI has a significant antithrombotic effect in vivo without increasing bleeding or impairing blood coagulation parameters.

Ir-CPI interferes with thrombus formation in mouse arterial thrombosis model.

To further investigate the antithrombotic in vivo effect of Ir-CPI on arterial thrombosis, we performed intravital videomicroscopy, using a skinfold chamber model in which a transparent window is surgically placed into the dorsal skin of NMRI mice to allow direct visualization and light excitation of the blood vessels. Thrombus generation in 1-mg/kg Ir-CPI–treated and untreated mice was initiated by i.v. injection of 10 mg/kg of rose bengal followed by 20 s of high light intensity exposition. In control mice, thrombus formation could be observed as soon as 30 min after light excitation and, 2 h later, blood flow was reduced or stopped in the major part of the chamber. However, in Ir-CPI–treated mice, no changes in the arterioles' aspect or flow could be recorded after 2 h (Fig. 7 A) or after 24 h (not depicted). Fluorescent microscopy confirmed these results (Videos 1–4) and provided additional flow velocity data with help of Cap Image, a computer-assisted image analysis program. Because flow velocity is not the same in each arteriole, results were expressed as a percentage of their own flow recorded before thrombus induction. Fig. 7 B shows an 86.2 ± 4.7% flow reduction in the control mice, whereas, in Ir-CPI-treated mice, the flow velocity remained unchanged.

DISCUSSION

Most of the antihemostatic mechanisms used by hematophagous parasites have evolved as adaptations to evade the vertebrate blood coagulation system (Mans et al., 2002). The importance of this selection pressure is illustrated by the wide range of strategies developed by these ectoparasites, enabling them to thwart primary hemostasis, clotting, and fibrinolysis during feeding (Ribeiro and Francischetti, 2003). Ticks are obligate hematophagous ectoparasites and, when they feed, their mouthparts cause extensive damage to the tissues surrounding the bite site as they break the vessels locally and establish a nutrition cavity rich in cells and host blood factors. These factors must, therefore, be inhibited if ticks are to accomplish their blood meal.

In vitro experiments showed that Ir-CPI considerably prolongs the aPTT (7.7-fold at 2.0 μM), which measures the intrinsic pathway of coagulation, without modifying the PT, which measures the extrinsic pathway, the thrombin time, which measures the conversion of fibrinogen to fibrin and its subsequent polymerization, or the RVV time, which measures the activation of FX into FXa and the subsequent coagulation steps. Coagulation contact phase factors may, therefore, be the targets of Ir-CPI. Surface plasmon resonance analysis and dot blot assays showed that Ir-CPI specifically binds to factors of the contact phase (namely, FXII, FXI, and kallikrein) but not to factors belonging to the common and TF pathways. In addition, Ir-CPI binds with a very high

affinity (Table I) to the activated form of the target enzymes and does not bind to the zymogenic form. This indicates that Ir-CPI does not block the activation of the target factor but, rather its action on the next factor in the clotting cascade. This was confirmed by showing that recombinant Ir-CPI protein inhibits the reciprocal activation of FXI, FXII, and prekallikrein in human plasma in a dose-dependent manner. Furthermore, Ir-CPI inhibits activation of these three factors in reconstituted systems (activation of a zymogen factor by an activated factor, activation of prekallikrein into kallikrein by FXIIa, and activation of FXI into FXIa by FXIIa) without affecting the amidolytic activity of these proteases. This was unexpected, as inhibitors belonging to the Kunitz-type serine protease inhibitor family (e.g., BPTI and TFPI) generally block the amidolytic activity of target proteases by binding the amino acid P1 of the inhibitors to the catalytic site of the enzyme (Laskowski and Kato, 1980). On the contrary, our results suggest that Ir-CPI does not directly interact with the site responsible for the amidolytic activity of FXIIa, FXIa, and kallikrein but probably acts on these factors by binding to an exosite, thereby preventing enzyme activity by steric hindrance. This action mechanism seems to be similar to that of two other anticoagulant factors: the Ixolaris protein, which is isolated from the tick *I. scapularis* (Francischetti et al., 2002), and bothrojaracin, which is isolated from the venom of the Brazilian snake jararaca (Zingali et al., 1993).

By binding to FXIIa, Ir-CPI prevents both activation of FXI into FXIa and activation of prekallikrein into kallikrein.

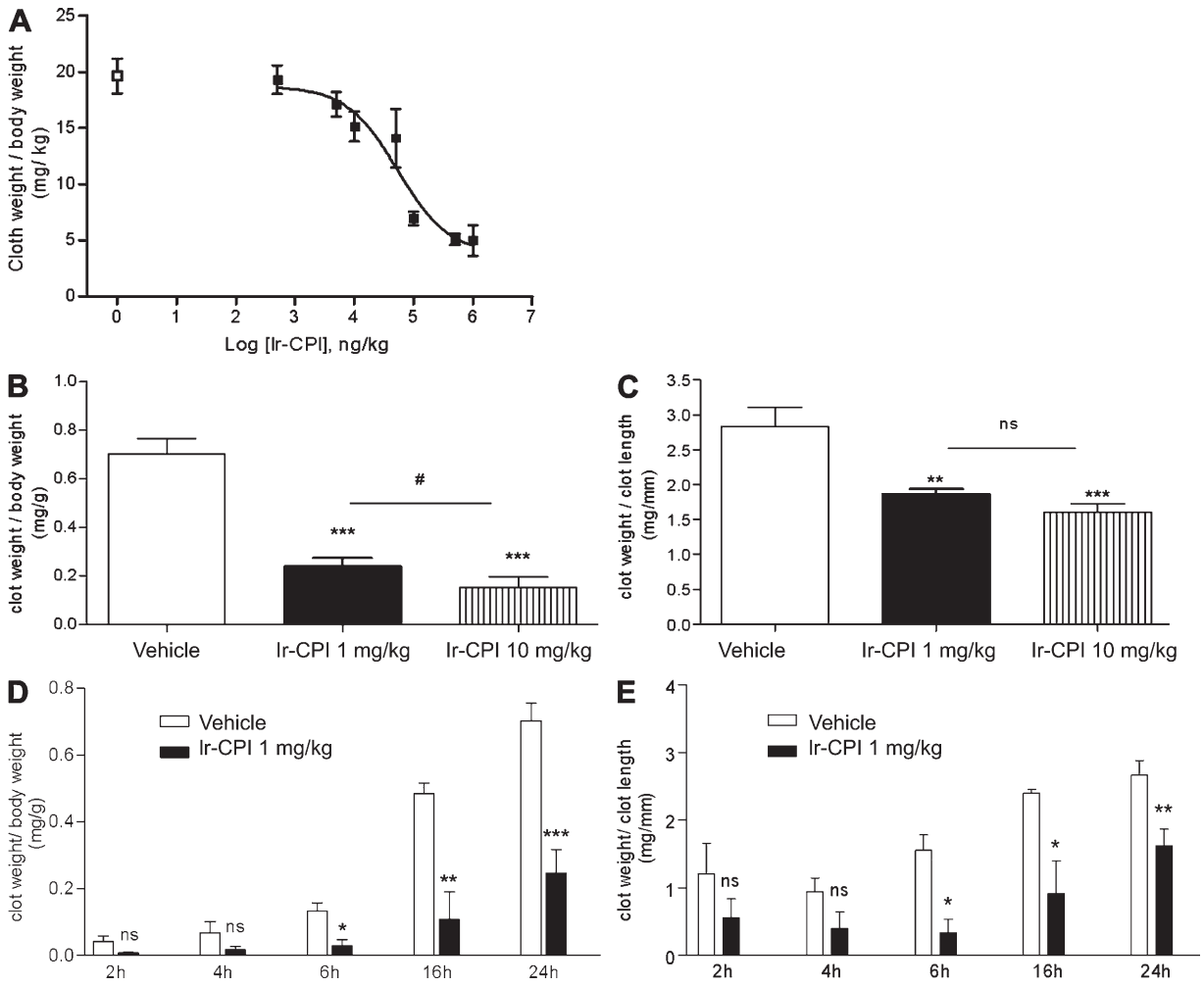

Figure 6. Effect of Ir-CPI on venous thrombosis in rats and mice. (A) Ir-CPI at the indicated doses was administered i.v. 5 min before induction of thrombosis by 10% $FeCl_3$ and complete stasis. The control group received PBS (□) instead of Ir-CPI (■). Each point represents the mean ± SEM for five or six animals. (B and C) Ir-CPI at the indicated doses was administered i.v. before IVC ligature. The control group received PBS instead of Ir-CPI. The thrombosed IVC fragments were harvested and weighed 24 h later. Results were expressed by dividing the thrombus weight with mouse weight (mg/g; B) or thrombus length (mg/mm; C). (D and E) Time-course experiments of clot formation. Results were expressed by dividing the thrombus weight with mouse weight (mg/g; D) or thrombus length (mg/mm; E). The experiment shown in A is representative of two independent experiments. The data shown in B–E are presented as the mean ± SEM of at least four independent experiments. *, $P \leq 0.05$; **, $P \leq 0.01$; ***, $P \leq 0.001$ (relative to vehicle); #, $P \leq 0.05$ (between 1 and 10 mg/kg Ir-CPI dose).

Table III. Hemostasis and coagulation in Ir-CPI treated mice

Inhibitors	aPTT	PT	Fibrinolysis	Bleeding effect (O.D. 450 nm)
	s	*s*	*min*	
PBS	21.7 ± 2.4	25.4 ± 1.6	26 ± 9.7	8.6 ± 3.3
Ir-CPI 1 mg/kg	25.8 ± 5.8	25.1 ± 0.1	25 ± 11.3	7.6 ± 4.7
Ir-CPI 10 mg/kg	39.8 ± 5.2[a]	27.5 ± 2.6	21 ± 4.6	14.5 ± 4.8
LMWH 0.5 mg/kg	47.5 ± 6.3[a]	28.9 ± 3.3	23 ± 5.0	>30.0 ± 0.0[a]

Values are mean ± SEM (n = 5 for each test). LMWH, low molecular weight heparin.
[a]$P < 0.05$, as compared to values observed in the control (PBS) by one-way ANOVA and Student's t test–Newman-Keuls test.

Likewise, by binding to FXIa, Ir-CPI prevents both activation of FXII into FXIIa and activation of FIX into FIXa. Moreover, Ir-CPI also has an affinity for kallikrein (Table I) so that it has an inhibitory effect on the kallikrein–kinin system as well as an immediate inhibitory effect on activation of FXII into FXIIa. Thus, the specificity of Ir-CPI for the activated factors initiating the contact phase alone is remarkable in that it only targets the contact phase during activation.

To better evaluate the potential anticoagulant effect of Ir-CPI in human plasma, we used the recently described thrombin generation method as a pharmacological tool (Robert et al., 2009). Thrombin generation, which is more sensitive to the action of anticoagulant (Prasa et al., 1997a,b), has long been known to be a valid physiological function test for investigating thrombin activity during the coagulation process (MacFarlane and Biggs, 1953; Pitney and Dacie, 1953). This test has major advantages in comparison with the classical PT or aPTT clotting assays. Only the initiation phase is investigated in the latter assay and its endpoint is plasma clotting, which occurs when the burst of thrombin generation has not yet taken place (Mann et al., 2003). Measurement of PT or aPTT therefore provides no information about the total amount of thrombin generated or the kinetics of the process. Moreover, in this test, a large and physiologically irrelevant excess of activator is used, leading to a massive activation of the coagulation cascade. Consequently, effective inhibitor concentrations must usually be relatively high. The results obtained with Ir-CPI confirm that this protein is a potent inhibitor of thrombin generation.

Contact phase defects are manifested by a prolongation of aPTT in vitro. However, deficiencies affecting these factors do not cause excessive bleeding (Colman, 1984). As an exception to this rule, FXI deficiency leads to mild bleeding after trauma or injury. This is in agreement with the suggestion that the main role of FXI is not the initiation of coagulation but the insurance of a positive-feedback mechanism ensuring the secondary production of thrombin, which is essential for efficient hemostasis (Gailani and Broze, 1991). A thrombophilia study confirmed this hypothesis. It showed that an increased level of FXI is a risk factor for thrombosis. It also suggested that FXI had a twofold role: secondary generation of thrombin and down-regulation of fibrinolysis via TAFI (Meijers et al., 2000). The ability of thrombin to activate FXI may also explain why FXII is not required for normal blood clotting in

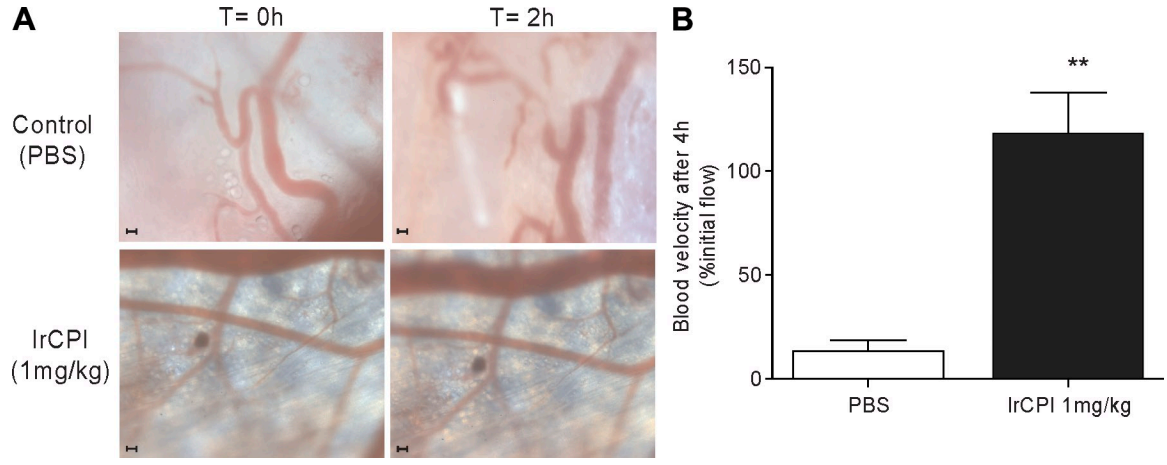

Figure 7. Intravital microscopy images from mouse dorsal skinfold window chambers illustrating the effect of Ir-CPI on high light intensity–induced thrombosis. (A) Representative images of microvessels of 1-mg/kg Ir-CPI–treated (bottom) and untreated (top) mice. The vessels after injection of 10 mg/kg of rose bengal but before high light intensity stimulation (time, 0) are shown on the left. The same vessels 2 h after high light intensity excitation (time, 2 h) are shown on the right. Representative images of five experiments are shown. Bars, 100 µm. (B) Bar graph showing changes in blood flow velocity in untreated and Ir-CPI–treated mice (n = 5). Results are expressed as a percentage of initial flow measured in each vessel. Data represent the mean ± SEM of results obtained from five independent experiments. **, $P < 0.01$.

vivo as shown in patients deficient for FXII. Similarly, Renné et al. (2005) showed that the coagulation balance of FXII KO mice is not disturbed in any way and is similar to that observed in wild-type mice. However, FXII KO mice are protected from thrombus formation, an essential element in venous and arterial thrombosis. In FXI-deficient mice, fibrin formation in ischemic vessels in the brain is reduced in comparison with wild-type mice, suggesting that the thrombosis-inducing effects of FXII are mediated through FXI and the contact phase (Renné et al., 2005, 2006; Colman, 2006; Kleinschnitz et al., 2006). Moreover, a recent study indicates that, in a plasma environment, thrombin or TF do not activate FXI, even in the presence of platelets (Pedicord et al., 2007). These results, together with the identification of an antithrombotic phenotype in FXII KO mice, suggest that FXI activation by the contact system may be physiologically relevant. Although differences may exist between mouse and human systems, FXII or FXI probably have similar roles during thrombosis in mice and in humans. These proteases may, therefore, provide attractive targets for the prevention or treatment of thromboembolic diseases with a minimal risk of therapy-associated bleeding (Gailani and Renné, 2007; Renné and Gailani, 2007). Kleinschnitz et al. (2006) used a synthetic inhibitor of FXIIa (Silverberg and Kaplan, 1982), D-Pro-Phe-Arg-CH_2Cl (PCK), to highlight FXIIa as a new drug target. However, the selectivity of this compound should be challenged. Indeed, it also inhibits in vitro the amidolytic activity of plasma kallikrein, plasmin, factor Xa, thrombin, TF/FVIIa, and urokinase. Moreover, the peptidic structure, as well as the alkylating behavior of the chloromethyl function, makes PCK unsuited for oral clinical use as anticoagulant agent (Kettner and Shaw, 1978; Robert et al., 2008).

We therefore evaluated the inhibitory effect of Ir-CPI on both venous and arterial thrombus formation in animal models closer to physiological venous and arterial thrombus formation. In venous models, thrombosis was induced by the infusion of a mixture of collagen and epinephrine into the jugular vein of the mouse, by ferric chloride and complete stasis of the posterior vena cava in the rat, and by complete stasis of the vena cava for 24 h in the mouse. Consistent with the results obtained with FXII-deficient mice (Renné et al., 2005), Ir-CPI seems to protect against collagen/epinephrine thromboembolism (20 and 26.7% of survivors at a dose of 1 and 10 mg/kg of Ir-CPI, respectively) without any effect on primary hemostasis, confirming that Ir-CPI does not inhibit the platelet adhesion/activation and aggregation processes. In the two other venous models, it was also shown that Ir-CPI reduced thrombus formation in a dose-dependant manner with an EC50 calculated in the rat of ~50 μg/kg and a maximum effect starting from 0.1 mg/kg (mean reduction of 71.0 ± 5.1% in the weight of the clot). Moreover, the clot weight/body weight ratio and the clot weight/clot length ratio were significantly lower in Ir-CPI–treated mice at a dose of 1 mg/kg than in untreated mice after 6, 16, and 24 h of stasis, whereas no difference was observed after 2 and 4 h, showing that Ir-CPI also impacts clot density. These data suggest that Ir-CPI acts mainly on clot propagation. This observation is consistent with the in vitro interactions of Ir-CPI with FXIIa, FXIa, and kallikrein, with these contact factors being mainly implicated in the clot propagation. The change in thrombus weight and density is probably related to the inhibitory effect of Ir-CPI on thrombin generation. Furthermore, the inhibitory effect of Ir-CPI on thrombus formation in the mouse model shows the efficacy of Ir-CPI over a 24-h period, confirming the results obtained in the rat showing the presence of ~41% of Ir-CPI 24 h after its i.v. injection. From the point of view of clotting physiology, the ex vivo values of aPTT, PT, and fibrinolysis times were unchanged at an Ir-CPI concentration of 0.1 mg/kg. At higher doses (1 mg/kg and 10 mg/kg), only the value of aPTT was significantly increased as it was observed with FXII-KO mice (Renné et al., 2005). Importantly, it should also be pointed out that the bleeding time of animals treated by Ir-CPI was not significantly changed even at the highest doses.

In the arterial model, thrombosis was induced by i.v. injection of rose bengal followed by high light intensity exposition. In Ir-CPI–treated mice, no changes in the arterioles' aspect or flow could be recorded after 2 h (Fig. 7 A) or after 24 h (not depicted). In addition, we observed a flow reduction in the control mice, whereas in Ir-CPI-treated mice, the flow velocity remained unchanged. Therefore, in these in vivo models used to study platelet recruitment and thrombus formation at sites of arteriole injury in Ir-CPI–treated mice, we observed a profound defect in the formation and stabilization of platelet-rich thrombi.

Although contact phase factors have long been considered to not be required for in vivo coagulation, recent studies show that mice genetically deprived of one of these factors are protected against the formation of both venous and arterial thrombi (Renné et al., 2005). Results obtained with the Ir-CPI protein confirm that a specific coagulation contact phase inhibitor is effective in animal thromboembolic models. Therefore, our study confirms the important role of contact phase factors in the coagulation propagation phase that causes the secondary generation of active thrombin. However, results obtained with the Ir-CPI protein do not exclude the possibility that the effects observed in vivo may result from the reciprocal inhibition of contact phase factors. These results could be the result of FXIa inhibiting the activation of FIX in the amplification phase, depending on the former's activation by thrombin.

The selection of anticoagulant therapy, whether for venous thromboembolism or arterial thrombosis (myocardial infarction or stroke), is based on how well the drug inhibits thrombosis and on the extent of the bleeding side effects (Colman, 2006). The discovery that FXII deficiency protects against thrombosis without causing spontaneous bleeding makes FXII a unique and attractive target for drug design (Gailani and Renné, 2007; Renné and Gailani, 2007). The data of the current study demonstrate that an exogenous molecule targeting the contact phase factors (FXII and FXI) can protect against the formation of a thrombus without altering

coagulation and bleeding times. Effectively, Ir-CPI has a dose-dependent protective action against thrombin-induced thromboembolism in four animal models without disturbing the clotting balance. At the effective doses, no effect was observed on aPTT and PT values, fibrinolysis time, or, remarkably, on bleeding time. To our knowledge, this is the first time that an inhibitor of the coagulation contact phase has been shown to protect against the formation of venous and arterial thrombi. Ir-CPI may, therefore, provide an important therapeutic tool by protecting patients at risk from diseases such as pulmonary embolism, cerebral ischemia, deep vein, and arterial thrombosis.

MATERIALS AND METHODS

Animals

Animal care and experimental procedures were performed in accordance with the Helsinki Declaration (Publication 85–23, revised 1985), local institutional guidelines (laboratory license LA 1500474), and the Belgian law of 14th August 1986, as well as the royal decree of the 14th of November 1993 on the protection of laboratory animals. Animal protocols were approved by the local ethic commission of the Université Libre de Bruxelles. Studies were performed using male Sprague-Dawley OFA rats weighing 250–300 g (Harlan) and 8-wk-old NMRI female mice weighing 20–25 g (Elevage Janvier).

Expression and purification of recombinant Ir-CPI in *Escherichia coli*

The coding region of Ir-CPI cDNA was cloned in frame with GST in the pGEX-6P-1 vector and transformed into *E. coli* strain BL21. Production of the recombinant protein was induced by the addition of 1 mM IPTG at 37°C for 2 h. After centrifugation of bacterial lysates prepared using a French press, the resulting supernatant, which contained the GST-Ir-CPI fusion protein, was incubated with Glutathione Sepharose High Performance (GE Healthcare). Ir-CPI was released by cleaving with PreScission protease according to the manufacturer's specifications and then purified to homogeneity by gel filtration chromatography using a HiLoad Superdex 75 column (GE Healthcare). Purified proteins were then tested for endotoxin contamination using the Limulus Amebocyte Lysate QCL-1000 kit (Cambrex). Endotoxin levels were <0.4 enzyme units/mg of protein in all preparations used. Samples containing endotoxin amounts superior to that threshold were loaded on Detoxi-Removal endotoxin gel columns according to the manufacturer's instructions (Thermo Fisher Scientific) to ensure the removal of endotoxins. This was followed by dialysis against buffers appropriate for the subsequent experiments. Protein concentrations in the endotoxin-purified batches were determined using a Micro BCA kit (Thermo Fisher Scientific) according to the manufacturer's instructions.

Primary hemostasis

Human blood samples were collected from healthy donors in 0.102-M trisodium citrate tubes (9:1 vol/vol). Global platelet function was measured on a PFA-100 machine (Siemens) with a collagen/epinephrine or collagen/ADP cartridge. The sample (1/10 protein in HBSS and 9/10 citrated whole blood) was aspirated through a capillary under steady high shear rates within 45 min of sample collection. Platelet plug formation was induced by the presence of the platelet agonists and the high shear rates, and this gradually occluded the aperture. The closure time was considered to be the time required to obtain full occlusion of the aperture. This time is called the closure time (CT) and is measured in seconds. The test is therefore a combined measure of platelet adhesion and aggregation. Platelet aggregation was performed using the impedance channel of a Whole Blood Lumi-Aggregometer (Chrono-Log Corporation; Ingerman-Wojenski and Silver, 1984). With this method, the electrical impedance between two fine electrodes immersed in the sample increases with platelet coating and aggregation on these electrodes after the addition of an agonist (collagen; Chrono-Log Corporation). Platelet aggregation was measured as the maximal per 10-min change in impedance.

Anticoagulant activity

The anticoagulant activities of Ir-CPI were determined by four coagulation tests using a Start8 coagulometer (Diagnostica Stago). Blood samples were collected in 3.8% trisodium citrate from healthy human donors, rats, and mice. Platelet-poor plasma (PPP) was obtained by further centrifugation at 4,000 *g* for 10 min.

aPTT. 25 µl of plasma and 25 µl Ir-CPI were preincubated for 2 min at 37°C. Mixtures were activated for 4 min with 25 µl actin FS (Siemens). Clotting was initiated by adding 50 µl of 25 mM $CaCl_2$.

PT. 25 µl of plasma and 25 µl Ir-CPI were preincubated for 2 min at 37°C. Mixtures were activated for 4 min with 25 µl innovin, 1/10 from human plasma or 1/100 from animal plasma (Siemens). The clotting reaction was started by adding 50 µl of 25 mM $CaCl_2$.

Russel viper venom time. 25 µl of plasma, 50 µl Hepes buffer (25 mM Hepes, 2% Glycine, and 145 mM NaCl, pH 7.35), and 25 µl Ir-CPI were preincubated for 2 min at 37°C. Clotting was initiated by the addition of 25 µl LA 1 (Siemens).

Thrombin time 25 µl of plasma, 50 µl Hepes buffer, and 25 µl Ir-CPI were preincubated for 2 min at 37°C. Clotting was initiated by the addition of 25 µl thrombin (Diagnostica Stago).

Determination of clot lysis times

Clot lysis times on PPP were determined as previously described (Boudjeltia et al., 2002).

Thrombin activity profiles

Materials. PPP reagent (5 pM TF and 4 µM PL in the final mixture), PPP LOW reagent (1 pM TF and 4 µM PL in the final mixture), and thrombin calibrator were purchased from Synapse BV. For each experiment, a fresh mixture of fluorogenic substrate/calcium chloride buffer solution was prepared as follows: 2,275 µl of buffer (20 mM Hepes, pH 7.35) containing 60 mg/ml of bovine serum albumin (Sigma-Aldrich) and 240 µl of 1 M calcium chloride were mixed with 60 µl of 100 mM DMSO solution of fluorogenic thrombin substrate (Z-Gly-Gly-Arg-AMC; Bachem). Actin FS was diluted 25-fold with distilled water.

Preparation of human plasma. Blood from healthy male volunteers, who were free from medication for at least 2 wk, was taken by venipuncture and collected into 0.105 M sodium citrate (9:1 vol/vol). PPP was obtained by centrifugation at room temperature for 10 min at 2,500 *g* and was used immediately after centrifugation.

Calibrated automated thrombin activity measurement. Thrombin activity measurement was performed using the previously reported CAT procedure (Hemker et al., 2003; Robert et al., 2009). In brief, 80 µl PPP, 10 µl PBS or Ir-CPI, and 20 µl PPP reagent, PPP LOW reagent, or diluted Actin FS were mixed in a 96-well microtiter plate (Immulon 2HB; Thermo Fisher Scientific) and incubated for 5 min at 37°C. The coagulation process was triggered by the addition of 20 µl of substrate/calcium chloride buffer at 37°C. A calibration condition was also realized. In this latter case, the same protocol as that described using PBS was followed, but the activator was replaced by 20 µl of thrombin calibrator. The reaction of fluorogenic thrombin substrate hydrolysis was monitored on a microplate fluorometer (Fluoroskan Ascent FL; Thermo Fisher Scientific) with a 390/460-nm (excitation/emission) filter set. Fluorescence was measured every 20 s for 60 min. The commercially available Thrombinoscope software (Synapse BV) automatically processed the acquired data to give thrombin activity profile curves and measurement parameters (lag time and Cmax). 10 Ir-CPI concentrations ranging from 0.001 to 9.077 µM were tested in each experiment in triplicate.

Assay of the inhibitory effect of Ir-CPI on coagulation factors

The inhibitory activity of Ir-CPI was examined on seven procoagulant serine proteases (plasma kallikrein, FXIIa, FXIa, FIXa, FXa, thrombin, and FVIIa) and two fibrinolytic serine proteases (t-PA and plasmin). Each serine protease was preincubated with Ir-CPI in a 1:5 molar ratio for 5 min at 37°C, followed by the addition of the appropriate chromogenic substrate (final concentration 0.5 mM). Final concentrations in a total volume of 200 µl in 96-microwell plates were the following: 3 nM kallikrein/S-2302, 62.5 nM FXIIa/S-2302, 31.25 nM FXIa/S2366, 500 nM FIXa/Spectrozyme FIXa, 10 nM FXa/S-2222, 35 nM thrombin/Spectrozyme TH, 100 nM FT-FVIIa/Spectrozyme FVIIa, 35 nM t-PA/Spectrozyme t-PA, and 30 nM plasmin/Spectrozyme PL. The kinetics of substrate hydrolysis were measured over 20 min. Chromogenic substrates S-2302, S-2366, and S-2222 were supplied by Chromogenix, and Spectrozyme FIXa, TH, FVIIa, t-PA, PL were obtained from American Diagnostica Inc.

Assay of the effects of Ir-CPI on contact system activation in plasma

The effects of Ir-CPI on the activation of the contact system in human plasma were assessed from the generation of activated contact factors (FXIa, FXIIa, and kallikrein). Human plasma was treated with acid to inactivate plasma serine protease inhibitors (De La Cadena et al., 1987) and then diluted 1:10 in buffer. 50 µl of diluted plasma was incubated with 20 µl of various concentrations of Ir-CPI for 5 min and then activated with 5 µl aPTT reagent (actin FS). After 10 min, a chromogenic substrate mixture at a final concentration of 0.5 mM and one or two inhibitors, 100 nM of Maize trypsin inhibitor or 50 µM kallistop, were added, and the amidolytic activity of the generated enzyme was determined at 405 nm for 3, 10, and 30 min for kallikrein, factor XIIa, and factor XIa, respectively. Sets of added chromogenic substrate and inhibitors were the following: S-2366, kallistop, and CTI for FXIa assay; S-2302 and kallistop for FXIIa assay; and S-2302 and CTI for kallikrein assay.

Effect of Ir-CPI in a reconstituted system

A reconstitution assay of the kallikrein–kininogen–kinin system was performed using purified coagulation factors (FXIIa and prekallikrein). 12.5 nM FXIIa was preincubated with Ir-CPI in Hepes buffer for 2 min at 37°C. 12.5 nM prekallikrein was added to the mixture, and then prekallikrein activation was started. After 10 min, chromogenic substrate S-2302 and CTI were added, and the increase in absorbance at 405 nm was recorded over 3 min. Reconstitution assays of the intrinsic coagulation pathway were performed using purified coagulation factors FXI/FXIa and FXII/FXIIa. The effect of Ir-CPI on the activation of FXI by FXIIa was tested by incubating 15 nM FXI, 60 nM FXIIa, and Ir-CPI for 10 min at 37°C. After incubation, substrate S-2366 was added and the increase in absorbance was measured. The effect of Ir-CPI on the activation of FXII by FXIa was tested by incubating 15 nM FXIa, 60 nM FXII, and Ir-CPI for 10 min at 37°C. After incubation, substrate S-2302 was added and the increase in absorbance was measured.

Binding analysis using surface plasmon resonance

The interaction between Ir-CPI and coagulation (HK, plasma prekallikrein, plasma kallikrein, FXII, FXIIa, FXI, FXIa, FIX, FIXa, FX, FXa, prothrombin, thrombin, and FVIIa) or fibrinolytic (t-PA, plasminogen, and plasmin) factors was monitored using a BIAcore X instrument (GE Healthcare). 15 µM Ir-CPI was immobilized on the surface of a CM5 sensor chip in 10 mM acetate buffer, pH 5.0, by the amine coupling procedure according to the manufacturer's instructions. 1,500 RU of immobilized Ir-CPI were used for the assay. To subtract the nonspecific component from the apparent binding response, a blank flow cell was prepared using the same immobilizing procedure without Ir-CPI. Binding analyses were performed using HBS buffer (10 mM Hepes, 150 mM NaCl 3 mM, and EDTA, pH 7.4, with 0.005% surfactant P20) as running buffer at 25°C. 100 µl of each 100-nM analyte was injected on the sensor chip at a flow rate of 70 µl/min. Association was monitored during an 84-s injection of analyte. Dissociation was monitored for 3 min after return to the running buffer. Regeneration of the sensor chip surface was achieved with a 15-µl pulse injection of 25 mM NaOH.

The kinetics of interactions between Ir-CPI and the four interacting factors were performed after a new immobilization of Ir-CPI. The quantity of Ir-CPI immobilized for measurements of kinetics was deliberately maintained at a low level (to ~200 RU) to avoid the problems of limitation of the reaction by the process of mass transport. Independence with respect to differences in flow of the initial rate of connection, measured by linear regression at the start of the kinetics after injections of analytes with increasing flows (30–70 µl/min), confirmed that the reactions were not limited by such a process. Interaction kinetics were determined for each analyte, with six different concentrations (from 5 nM to 300 nM). Binding data were analyzed using BIA evaluation software to determine the kinetic constants. The specificity of the reaction was evaluated using the GST protein (~1,000 RU immobilized on the surface of the sensor chip) as negative control.

Determination of radioactivity of ^{125}I–Ir-CPI in rat blood

^{125}I-labeled Ir-CPI was prepared by iodination with [^{125}I] sodium iodide in 20 mCi/mg of protein, using IODO-BEADS Iodination Reagent (Thermo Fisher Scientific), according to the manufacturer's instructions. Free iodide was removed by extensive gel filtration on Sephadex G10.

The in vivo distribution of ^{125}I–Ir-CPI in rat blood was evaluated after i.v. administration. Samples containing 10×10^6 cpm were resuspended in 200 µl of PBS and administered to rats. Blood was collected after 3, 20, 40, or 60 h by cardiac puncture in 3.8% trisodium citrate. Plasma was obtained by centrifugation, and aliquots of 500 µl were placed in glass test tubes. Radioactivity was determined in a gamma counter.

Ex vivo effect of Ir-CPI on aPTT, PT, and fibrinolysis

Ir-CPI was administered i.v. to rats and mice, and blood was collected after 5 min by cardiac puncture in 3.8% trisodium citrate. PPP was obtained by centrifugation at 4,000 *g* for 10 min. The aPTT, PT, and fibrinolysis times were measured using theses procedures.

Collagen/epinephrine-induced pulmonary thromboembolism

20–25-g C57BL/6J mice were anesthetized by i.p. injection of a mixture of 80 mg/kg ketamine and xylazine (5 mg/kg). 1–10 mg/kg Ir-CPI or vehicle was injected in the iliac vein 5 min before challenge. A mixture of 0.8 mg/kg collagen and 60 µg/kg epinephrine was then injected into the jugular vein. Platelet counts were determined by flow cytometry.

Histopathologic analyses

C57BL/6J mice were killed and lungs were fixed at 4°C for 24 h in buffered 4% formaldehyde. Tissues were dehydrated and embedded in paraffin, cut into 5-µm sections, and stained with Mayer's hematoxylin and eosin (Sigma-Aldrich).

Complete stasis combined with vessel injury induced venous thrombosis model in the rat

Thrombus formation was induced by a combination of complete stasis and vessel injury by ferric chloride according to the modification of the method described by Peternel et al. (2005). Rats were anesthetized i.p. with 70 mg/kg pentobarbital sodium. The abdomen was opened by making an incision along the linea alba toward the sternum, followed by exposition of the posterior vena cava. Surgical threads, 1 cm apart, were placed loosely around the vena cava beneath the renal veins and above the bifurcation of the iliac veins to form a snare. Complete stasis was induced in the posterior vena cava by tightening the downstream snare firmly around the posterior vena cava. Simultaneously, a piece of filter paper (0.3 × 0.8 cm) saturated with 10% wt/vol ferric chloride solution was applied to the external surface of the posterior vena cava caudally of the ligature for 10 min, 10 min after the removal of the filter paper, the upstream snare was firmly tightened around the posterior vena cava, and the rat was then euthanized. The ligated venous segment was excised and the thrombus was removed and immediately weighed after blotting off excess blood. Results were expressed in milligrams of thrombus per kilogram of rat body weight. Ir-CPI (0.5–1,000 µg/kg, corresponding to ~2 nM to 4 µM) or vehicle were injected in the left femoral vena 5 min before the induction of the thrombus formation.

Experimental venous thrombosis induced by complete stasis in mice

NMRI female mice (20–25 g) were anesthetized with a mixture of 80 mg/kg ketamine and 10–16 mg/kg xylazine. Aseptic laparotomy was performed; the IVC was isolated and ligated below the renal veins. Major side branches were also ligated. Insides were replaced and the midline incision was closed. Ir-CPI (1 and 10 mg/kg, corresponding to ~3 and 30 μM) or vehicle was injected in the caudal vein 5 min before surgery. The animals were sacrificed 2, 4, 6, 16, and 24 h after thrombosis induction, and thrombosed IVC fragments were harvested and weighed. Results were expressed as thrombus weight over thrombus length (milligrams/millimeters) or mouse weight (milligrams/grams).

Dorsal skinfold window chamber

NMRI mice weighing between 25 and 30 g were anesthetized with an intraperitoneal injection of 80 mg/kg ketamine and 10-16 mg/kg xylazine and i.v. injected with 0.05 mg/kg buprenorphine. Under sterile conditions, a 12-mm circular section of skin was surgically excised from the dorsal side of the mouse, exposing the microcirculation. A dorsal skinfold window chamber was then surgically implanted around the dissected circle of tissue. After the window chamber had been sutured to the skin, the exposed microcirculation was carefully covered with a round cover glass (Fukumura and Jain, 2008; Makale, 2008). Mice were allowed 6 d to recover from surgery before thrombosis induction.

Platelet labeling for intravital microscopy

Platelets were prepared as described previously (Bonnefoy et al., 2006). In brief, platelet-rich plasma was obtained from NMRI mouse blood upon addition of 0.2 vol acid-dextrose-citrate (93 mM Na_3-citrate, 7 mM citric acid, and 0.14 M dextrose, pH 6.5) and subsequent centrifugation at 800 *g* for 5 min. 500×10^9 platelets/liter were resuspended in Tyrode's buffer and incubated for 15 min at 37°C with 10 μg/ml calcein.

Intravital videomicroscopy of thrombus formation

NMRI mice with dorsal skinfold window chambers were anesthetized with a mixture of 80 mg/kg ketamine and 10–16 mg/kg xylazine. After i.v. injection of 10 mg/kg of rose bengal, the window chamber was exposed for 20 s to highlight intensity (bluephase 16i; Ivoclar Vivadent, Inc.) and thrombi generation was recorded (Westrick et al., 2007). For in vivo fluorescence microscopy, FITC-conjugated 2,000-kD dextran and labeled platelets were i.v. injected and videotaped images were evaluated off-line using a computer-assisted image analysis program (Cap Image 7.1; H. Zeintl, Heidelberg, Germany).

Bleeding effect

Both rat and mouse tail transection models were used to evaluate the effect of Ir-CPI on bleeding time. Animals were anesthetized as indicated in previous sections and Ir-CPI was administered i.v. into the vena cava. In the case of rats, the tail was cut 3 mm from the tip after 5 min, and was carefully immersed in 40 ml of distilled water warmed at 37°C. The hemoglobin content of the aqueous solution (absorbance at 540 nm) was used to estimate blood loss. Appropriate controls (i.v. injection of PBS) were run in parallel. In the case of mice, bleeding was monitored by gently absorbing the bead of blood with a filter paper at 15-s intervals without touching the wound. Bleeding was stopped manually if it continued for 30 min.

Statistics

Data were analyzed by one way analysis of variance (ANOVA) with a post-hoc Newman-Keuls multiple comparison test.

Online supplemental material

Fig. S1 shows dot-blot assays in which coagulation factors (zymogen and their activated form; 15–100 ng/protein) were spotted on nitrocellulose membrane. Video 1 shows real-time microscopy video of microvessels of mouse before thrombosis induction. Video 2 shows a real-time light microscopy video of embolization in a microvessel 2 h after thrombosis induction. Video 3 shows a real-time microscopy video of microvessels of an Ir-CPI–treated mouse before thrombosis induction. Video 4 shows a real-time microscopy video of microvessels of an Ir-CPI–treated mouse 2 h after thrombosis induction. Online supplemental material is available at http://www.jem.org/cgi/content/full/jem.20091007/DC1.

We thank Louis Delhaye for his excellent technical assistance and handling and maintenance of mice and rats. We are thankful to Professor Michel Vanhaeverbeek and Michel Brossard and Dr. Claudine Fraipont for helpful discussions. We thank Dr. Michel Pétein for histopathologic analyses. Finally, we are thankful to Dr. Pierre Sonveaux and Dr. Caroline Bouzin for their excellent methodological assistance in the implantation of dorsal skinfold window chambers and videomicroscopy, respectively, and Dr. H. Zeintl, who allowed us to use the Cap Image 7.1 software (Ingenieurbüro Dr. Zeintl, Heidelberg, Germany).

L. Vanhamme is a Senior Research associate at the Belgian National fund for scientific research. L. Vanhamme and E. Godfroid should be considered as co-senior authors. C. Dessy is a Research associate at the Belgian National fund for scientific research. This work was supported by grants from the Walloon Region (convention 215.107 and 215.055) and the FRFC (grants 9.4519.98, 2.4511.06, and 2.4560.09). Research in the laboratory was also supported by grants from the Fonds Jean Brachet and the Fonds van Buuren.

The authors have no conflicting financial interests.

Submitted: 7 May 2009
Accepted: 9 September 2009

REFERENCES

Bauer, K.A., B.L. Kass, H. ten Cate, J.J. Hawiger, and R.D. Rosenberg. 1990. Factor IX is activated in vivo by the tissue factor mechanism. *Blood*. 76:731–736.

Bonnefoy, A., K. Daenens, H.B. Feys, R. De Vos, P. Vandervoort, J. Vermylen, J. Lawler, and M.F. Hoylaerts. 2006. Thrombospondin-1 controls vascular platelet recruitment and thrombus adherence in mice by protecting (sub)endothelial VWF from cleavage by ADAMTS13. *Blood*. 107:955–964. doi:10.1182/blood-2004-12-4856

Boudjeltia, K.Z., P. Cauchie, C. Remacle, M. Guillaume, D. Brohée, J.L. Hubert, and M. Vanhaeverbeek. 2002. A new device for measurement of fibrin clot lysis: application to the euglobulin clot lysis time. *BMC Biotechnol*. 2:8. doi:10.1186/1472-6750-2-8

Bouma, B.N., and J.H. Griffin. 1977. Human blood coagulation factor XI. Purification, properties, and mechanism of activation by activated factor XII. *J. Biol. Chem*. 252:6432–6437.

Brossard, M., and S.K. Wikel. 2004. Tick immunobiology. *Parasitology*. 129:S161–S176. doi:10.1017/S0031182004004834

Cochrane, C.G., S.D. Revak, and K.D. Wuepper. 1973. Activation of Hageman factor in solid and fluid phases. A critical role of kallikrein. *J. Exp. Med*. 138:1564–1583. doi:10.1084/jem.138.6.1564

Colman, R.W. 1984. Surface-mediated defense reactions. The plasma contact activation system. *J. Clin. Invest*. 73:1249–1253. doi:10.1172/JCI111326

Colman, R.W. 2006. Are hemostasis and thrombosis two sides of the same coin? *J. Exp. Med*. 203:493–495. doi:10.1084/jem.20060217

Davie, E.W., and O.D. Ratnoff. 1964. Waterfall sequence for intrinsic blood clotting. *Science*. 145:1310–1312. doi:10.1126/science.145.3638.1310

De La Cadena, R.A., C.F. Scott, and R.W. Colman. 1987. Evaluation of a microassay for human plasma prekallikrein. *J. Lab. Clin. Med*. 109:601–607.

Dunn, J.T., and A.P. Kaplan. 1982. Formation and structure of human Hageman factor fragments. *J. Clin. Invest*. 70:627–631. doi:10.1172/JCI110656

Dunn, J.T., M. Silverberg, and A.P. Kaplan. 1982. The cleavage and formation of activated human Hageman factor by autodigestion and by kallikrein. *J. Biol. Chem*. 257:1779–1784.

Francischetti, I.M., J.G. Valenzuela, J.F. Andersen, T.N. Mather, and J.M. Ribeiro. 2002. Ixolaris, a novel recombinant tissue factor pathway inhibitor (TFPI) from the salivary gland of the tick, *Ixodes scapularis*: identification of factor X and factor Xa as scaffolds for the inhibition of factor VIIa/tissue factor complex. *Blood*. 99:3602–3612. doi:10.1182/blood-2001-12-0237

Fukumura, D., and R.K. Jain. 2008. Imaging angiogenesis and the microenvironment. *APMIS*. 116:695–715. doi:10.1111/j.1600-0463.2008.01148.x

Gailani, D., and G.J. Broze Jr. 1991. Factor XI activation in a revised model of blood coagulation. *Science*. 253:909–912. doi:10.1126/science.1652157

Gailani, D., and T. Renné. 2007. The intrinsic pathway of coagulation: a target for treating thromboembolic disease? *J. Thromb. Haemost.* 5:1106–1112. doi:10.1111/j.1538-7836.2007.02446.x

Ghebrehiwet, B., B.P. Randazzo, J.T. Dunn, M. Silverberg, and A.P. Kaplan. 1983. Mechanisms of activation of the classical pathway of complement by Hageman factor fragment. *J. Clin. Invest.* 71:1450–1456. doi:10.1172/JCI110898

Hemker, H.C., P. Giesen, R. Al Dieri, V. Regnault, E. de Smedt, R. Wagenvoord, T. Lecompte, and S. Béguin. 2003. Calibrated automated thrombin generation measurement in clotting plasma. *Pathophysiol. Haemost. Thromb.* 33:4–15. doi:10.1159/000071636

Ingerman-Wojenski, C.M., and M.J. Silver. 1984. A quick method for screening platelet dysfunctions using the whole blood lumi-aggregometer. *Thromb. Haemost.* 51:154–156.

Josso, F., and O. Prou-Wartelle. 1965. Interaction of tissue factor and factor VII at the earliest phase of coagulation. *Thromb. Diath. Haemorrh. Suppl.* 17:35–44.

Kaplan, A.P., and K.F. Austen. 1971. A prealbumin activator of prekallikrein. II. Derivation of activators of prekallikrein from active Hageman factor by digestion with plasmin. *J. Exp. Med.* 133:696–712. doi:10.1084/jem.133.4.696

Kaplan, A.P., K. Joseph, and M. Silverberg. 2002. Pathways for bradykinin formation and inflammatory disease. *J. Allergy Clin. Immunol.* 109:195–209. doi:10.1067/mai.2002.121316

Kettner, C., and E. Shaw. 1978. Synthesis of peptides of arginine chloromethyl ketone. Selective inactivation of human plasma kallikrein. *Biochemistry*. 17:4778–4784. doi:10.1021/bi00615a027

Kisiel, W., K. Fujikawa, and E.W. Davie. 1977. Activation of bovine factor VII (proconvertin) by factor XIIa (activated Hageman factor). *Biochemistry*. 16:4189–4194. doi:10.1021/bi00638a009

Kleinschnitz, C., G. Stoll, M. Bendszus, K. Schuh, H.U. Pauer, P. Burfeind, C. Renné, D. Gailani, B. Nieswandt, and T. Renné. 2006. Targeting coagulation factor XII provides protection from pathological thrombosis in cerebral ischemia without interfering with hemostasis. *J. Exp. Med.* 203:513–518. doi:10.1084/jem.20052458

Kurachi, K., and E.W. Davie. 1977. Activation of human factor XI (plasma thromboplastin antecedent) by factor XIIa (activated Hageman factor). *Biochemistry*. 16:5831–5839. doi:10.1021/bi00645a030

Laskowski, M. Jr., and I. Kato. 1980. Protein inhibitors of proteinases. *Annu. Rev. Biochem.* 49:593–626. doi:10.1146/annurev.bi.49.070180.003113

Leboulle, G., C. Rochez, J. Louahed, B. Ruti, M. Brossard, A. Bollen, and E. Godfroid. 2002. Isolation of *Ixodes ricinus* salivary gland mRNA encoding factors induced during blood feeding. *Am. J. Trop. Med. Hyg.* 66:225–233.

MacFarlane, R.G. 1964. An enzyme cascade in the blood clotting mechanism, and its function as a biochemical amplifier. *Nature*. 202:498–499. doi:10.1038/202498a0

MacFarlane, R.G., and R. Biggs. 1953. A thrombin generation test; the application in haemophilia and thrombocytopenia. *J. Clin. Pathol.* 6:3–8. doi:10.1136/jcp.6.1.3

Makale, M. 2008. Chapter 8. Noninvasive imaging of blood vessels. *Methods Enzymol.* 444:175–199. doi:10.1016/S0076-6879(08)02808-5

Mandle, R.J. Jr., and A.P. Kaplan. 1979. Hageman-factor-dependent fibrinolysis: generation of fibrinolytic activity by the interaction of human activated factor XI and plasminogen. *Blood*. 54:850–862.

Mann, K.G., K. Brummel, and S. Butenas. 2003. What is all that thrombin for? *J. Thromb. Haemost.* 1:1504–1514. doi:10.1046/j.1538-7836.2003.00298.x

Mans, B.J., A.I. Louw, and A.W. Neitz. 2002. Evolution of hematophagy in ticks: common origins for blood coagulation and platelet aggregation inhibitors from soft ticks of the genus *Ornithodoros*. *Mol. Biol. Evol.* 19:1695–1705.

Meijers, J.C., W.L. Tekelenburg, B.N. Bouma, R.M. Bertina, and F.R. Rosendaal. 2000. High levels of coagulation factor XI as a risk factor for venous thrombosis. *N. Engl. J. Med.* 342:696–701. doi:10.1056/NEJM200003093421004

Moreau, M.E., N. Garbacki, G. Molinaro, N.J. Brown, F. Marceau, and A. Adam. 2005. The kallikrein-kinin system: current and future pharmacological targets. *J. Pharmacol. Sci.* 99:6–38. doi:10.1254/jphs.SRJ05001X

Osterud, B., and S.I. Rapaport. 1977. Activation of factor IX by the reaction product of tissue factor and factor VII: additional pathway for initiating blood coagulation. *Proc. Natl. Acad. Sci. USA*. 74:5260–5264. doi:10.1073/pnas.74.12.5260

Pauer, H.U., T. Renné, B. Hemmerlein, T. Legler, S. Fritzlar, I. Adham, W. Müller-Esterl, G. Emons, U. Sancken, W. Engel, and P. Burfeind. 2004. Targeted deletion of murine coagulation factor XII gene-a model for contact phase activation in vivo. *Thromb. Haemost.* 92:503–508.

Pedicord, D.L., D. Seiffert, and Y. Blat. 2007. Feedback activation of factor XI by thrombin does not occur in plasma. *Proc. Natl. Acad. Sci. USA*. 104:12855–12860. doi:10.1073/pnas.0705566104

Peternel, L., G. Drevensek, M. Cerne, A. Stalc, M. Stegnar, and M.V. Budihna. 2005. Evaluation of two experimental venous thrombosis models in the rat. *Thromb. Res.* 115:527–534. doi:10.1016/j.thromres.2004.10.007

Pitney, W.R., and J.V. Dacie. 1953. A simple method of studying the generation of thrombin in recalcified plasma; application in the investigation of haemophilia. *J. Clin. Pathol.* 6:9–14. doi:10.1136/jcp.6.1.9

Prasa, D., L. Svendsen, and J. Stürzebecher. 1997a. The ability of thrombin inhibitors to reduce the thrombin activity generated in plasma on extrinsic and intrinsic activation. *Thromb. Haemost.* 77:498–503.

Prasa, D., L. Svendsen, and J. Stürzebecher. 1997b. Inhibition of thrombin generation in plasma by inhibitors of factor Xa. *Thromb. Haemost.* 78:1215–1220.

Radcliffe, R., A. Bagdasarian, R. Colman, and Y. Nemerson. 1977. Activation of bovine factor VII by hageman factor fragments. *Blood*. 50:611–617.

Renné, T., and D. Gailani. 2007. Role of Factor XII in hemostasis and thrombosis: clinical implications. *Expert Rev. Cardiovasc. Ther.* 5:733–741. doi:10.1586/14779072.5.4.733

Renné, T., M. Pozgajová, S. Grüner, K. Schuh, H.-U. Pauer, P. Burfeind, D. Gailani, and B. Nieswandt. 2005. Defective thrombus formation in mice lacking coagulation factor XII. *J. Exp. Med.* 202:271–281. doi:10.1084/jem.20050664

Renné, T., B. Nieswandt, and D. Gailani. 2006. The intrinsic pathway of coagulation is essential for thrombus stability in mice. *Blood Cells Mol. Dis.* 36:148–151. doi:10.1016/j.bcmd.2005.12.014

Revak, S.D., C.G. Cochrane, and J.H. Griffin. 1977. The binding and cleavage characteristics of human Hageman factor during contact activation. A comparison of normal plasma with plasmas deficient in factor XI, prekallikrein, or high molecular weight kininogen. *J. Clin. Invest.* 59:1167–1175. doi:10.1172/JCI108741

Ribeiro, J.M., and I.M. Francischetti. 2003. Role of arthropod saliva in blood feeding: sialome and post-sialome perspectives. *Annu. Rev. Entomol.* 48:73–88. doi:10.1146/annurev.ento.48.060402.102812

Robert, S., C. Bertolla, B. Masereel, J.M. Dogné, and L. Pochet. 2008. Novel 3-carboxamide-coumarins as potent and selective FXIIa inhibitors. *J. Med. Chem.* 51:3077–3080. doi:10.1021/jm8002697

Robert, S., J. Ghiotto, B. Pirotte, J.L. David, B. Masereel, L. Pochet, and J.M. Dogné. 2009. Is thrombin generation the new rapid, reliable and relevant pharmacological tool for the development of anticoagulant drugs? *Pharmacol. Res.* 59:160–166. doi:10.1016/j.phrs.2008.12.003

Silverberg, M., and A.P. Kaplan. 1982. Enzymatic activities of activated and zymogen forms of human Hageman factor (factor XII). *Blood*. 60:64–70.

Silverberg, M., J.T. Dunn, L. Garen, and A.P. Kaplan. 1980. Autoactivation of human Hageman factor. Demonstration utilizing a synthetic substrate. *J. Biol. Chem.* 255:7281–7286.

Steen, N.A., S.C. Barker, and P.F. Alewood. 2006. Proteins in the saliva of the *Ixodida* (ticks): pharmacological features and biological significance. *Toxicon*. 47:1–20. doi:10.1016/j.toxicon.2005.09.010

Tankersley, D.L., and J.S. Finlayson. 1984. Kinetics of activation and autoactivation of human factor XII. *Biochemistry*. 23:273–279. doi:10.1021/bi00297a016

von dem Borne, P.A., J.C. Meijers, and B.N. Bouma. 1995. Feedback activation of factor XI by thrombin in plasma results in additional formation of thrombin that protects fibrin clots from fibrinolysis. *Blood*. 86:3035–3042.

Westrick, R.J., M.E. Winn, and D.T. Eitzman. 2007. Murine models of vascular thrombosis (Eitzman series). *Arterioscler. Thromb. Vasc. Biol.* 27:2079–2093. doi:10.1161/ATVBAHA.107.142810

Yarovaya, G.A., T.B. Blokhina, and E.A. Neshkova. 2002. Contact system. New concepts on activation mechanisms and bioregulatory functions. *Biochemistry (Mosc.)*. 67:13–24. doi:10.1023/A:1013991828598

Zingali, R.B., M. Jandrot-Perrus, M.C. Guillin, and C. Bon. 1993. Bothrojaracin, a new thrombin inhibitor isolated from *Bothrops jararaca* venom: characterization and mechanism of thrombin inhibition. *Biochemistry*. 32:10794–10802. doi:10.1021/bi00091a034